Springer

Journal of Mechanical Science and Technology

Journal of Mechanical Science and Technology 23 (2009) 2514~2520

www.springerlink.com/content/1738-494x
DOI 10.1007/s12206-009-0701-0

The measurement of thermal conductivities using the photothermal deflection method for thin films with varying thickness †

H. J. Kim*, J. H. Kim[1], P. S. Jeon[2] and J. Yoo[2]

[1]*Division of Mechanical Engineering, Ajou University*
[2]*KIBO Technology Fund*

(Manuscript Received February 18, 2008; Revised January 29, 2009; Accepted June 24, 2009)

Abstract

This study considers non-contact methods that obviate the causes of measurement error, such as thermal contact resistance and the unnecessary destruction of samples. Among the methods, the photothermal deflection method has been adopted and developed to measure the thermal conductivities of thin-film materials. To apply the developed method for thin films, bi-layered materials are manufactured by depositing the film on Corning 7740 glass plates. The study also investigates the optimal modulation frequency, as related to the thermal diffusion length of the sample, for measuring thermal conductivities of thin films.. Aluminum, TiO_2, and Si_3N_4 films with micro/nanometer thickness were selected as the objects for measurement; the thermal conductivities of these films were experimentally measured. Samples of thickness ranging from 1 ㎛ to 200 ㎚ were prepared to measure the variations in thermal conductivities with thickness. It was observed that the thermal conductivity in submicroscale films decreased as the thickness was reduced.

Keywords: Photothermal deflection method, Thermal conductivity; Thin film

1. Introduction

Micro/nano-techniques have been developed recently. This development strongly calls for research that finds new materials with excellent thermal properties as well as research that accurately identifies the thermal properties of microscale materials. Accordingly, techniques in measuring thermal properties are becoming increasingly important: these chniques are classified into contact and noncontact methods.

Contact methods include the direct electric heating method [1-3], the pulse electric heating method [4-6], laser calorimetry [7], and the 3-Omega method [8], which are among the most recently used, besides other methods. Noncontact methods include the ultrasonic wave laser heating method [9, 10], the photo acoustic method [7], the laser flash method [11], and photothermal methods [7]. Since they largely depend on direct contact between samples and a detector, contact methods can cause measurement errors through the destruction of samples and through thermal resistance. Furthermore, they cannot be applied to all objects and may require special treatment of samples for measurement.

In non-contact methods, there is no direct contact between samples, a detector, or the destruction of samples. These methods are not associated with accidental errors because they indirectly measure the physical phenomenon caused in the samples by the heat source. Photothermal methods, which measure the physical phenomena of the inner part of the sample, the surface of the sample, and the adjacent air layer, are the representative noncontact methods.

For single-layered samples, Salazar et al. [12, 13] developed equations of thermal diffusivity for the application of the photothermal deflection method. They presented empirical equations using the relationship between the gradient of the transverse phase

† This paper was recommended for publication in revised form by Associate Editor Dongsik Kim
*Corresponding author. Tel.: +82 52 259 2282, Fax.: +82 52 259 1680
E-mail address: kkahn@ulsan.ac.kr
© KSME & Springer 2009

difference and the thermal diffusion length. Jeon et al. [14] proposed a two-dimensional, analytical model for single-layered samples as well as an equation that can determine thermal diffusivity by using the transverse and normal phase curves. Lee et al. [15] suggested a two-dimensional, analytical model for single- and multi-layered samples and measured the thermal conductivities of optically thick materials, such as metal film and Si wafer. Chen et al. [16] measured Si samples with a microscale structure on the surface.

Despite all these studies, research has not sufficiently specified either the optimal experimental conditions for measurement or accurate data on the variation of thermal properties with thickness at the microscale, hence the importance of this study, in which we develop a measurement technique and measure the thermal conductivities of submicroscale, thin film materials. In addition, for each material, we use the photothermal deflection method to study the change in thermal conductivity with decreasing thickness.

2. Theory and principle

Thermal conduction in solid materials usually occurs through the vibration of phonons and electrons. Phonon describes the abnormal phenomenon of specific heat for solid materials at low temperatures. The lattice vibration and energy that are quantized to the acoustic wave that is propagated in the material are called phonons. In solids with a lattice structure, heat energy is accumulated as vibration energy and transferred to the adjacent phonon. In metals, this transfer comes with the vibration of electrons. When the characteristic length of the sample is thinner than the microscale, the boundary surface interferes with the vibration of phonons or electrons. As the characteristic length of the sample approaches the mean free path of the material, the effect on the thickness becomes greater. This phenomenon affects the thermal properties of the material.

The photothermal effect considered in this study is the physical change that occurs when absorbed light energy is transformed to heat energy. When the surface of the sample is irradiated by a laser beam, the energy of photons is transferred to the sample, causing the phonons or electrons in the sample to vibrate. Subsequently, the propagation of the vibration of phonons or electrons causes heat transfer.

Fig. 1 schematically shows the principle of the pho

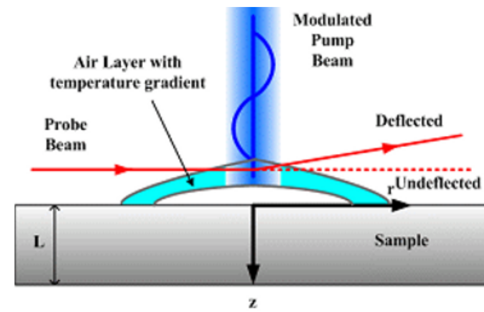

Fig. 1. Measurement principle of the photothermal deflection method.

tothermal deflection method.. The Fig. show that when the modulated pump beam is incident upon the surface of the sample, energy is absorbed by the sample, which, in turn, causes an increase in temperature. The change in the temperature of the sample induces a density gradient in the adjacent air layer, causing a change in the refractive index of the air layer. The change in the refractive index deflects the probe beam in which the optical path is parallel to the surface of the sample, without heating through the pump beam. This method is called the transverse photothermal deflection method. The deflection angle (Φ) of the probe beam is presented in Eq. (1) [12, 17].

$$\Phi = \int_{path} \frac{1}{n}\left(\frac{\partial n}{\partial T}\right)\nabla_t T(r,z,t)ds \tag{1}$$

Since the pump beam is modulated as shown in Fig. 1, the temperature-gradient of the air layer is also modulated with the same frequency as that of the modulated pump beam. However, the energy through heating by the pump-beam needs a finite time to diffuse; hence, a phase difference occurs between the modulated pump beam and the deflected probe beam. The photothermal deflection method experimentally measures the phase differences, which show different values in accordance with the thermal properties of the sample materials.

To evaluate thermal properties (specifically, thermal conductivity in this study), phase differences are calculated with iterative thermal conductivities; then, the measured phase differences are matched with theoretical values.

Fig. 2 describes the coordinates for theoretical analysis of the transverse photothermal deflection method.. To obtain Eq. (1) for the deflection angle,

temperature analysis of the air layer adjacent to the sample should be conducted. Fig. 3 is the schematic of the multi-layer model. Regions 0 and 3 are air layers, which do not absorb the optical energy, while regions 1 and 2 are the film layer and the substrate, respectively. The temperature distributions for the four regions can be obtained from two-dimensional heat equations [14].

$$\nabla^2 T_i - \frac{1}{\alpha_i}\frac{\partial T_i}{\partial t} = -\frac{1}{k_i} Q_i \qquad (i = 0, 1, 2, 3) \quad (2)$$

$$Q_1(r,z,t) = \frac{\lambda_1 P_0 (1-R_1)}{4\pi a^2} e^{-r^2/a^2 - \lambda z}[1+\cos(\omega t)] \quad (3a)$$

$$Q_2(r,z,t) = \frac{\lambda_2 P_0 (1-R_1)(1-R_2)}{4\pi a^2} e^{-r^2/a^2 - \lambda_2 (z-L_1)} \times e^{-\lambda_1 L_1}[1+\cos(\omega t)] \quad (3b)$$

The boundary conditions for the above governing equations are shown as Eq. (4). The heat flux and temperature are constant at z=0, L_1, and L_1+L_2.. Because the rise in the temperature of the specimen caused by the pump beam is negligible, the transfer of heat through either convection or radiation is not considered [18].

$$\begin{aligned} &T_0\big|_{z=0} = T_1\big|_{z=0} \\ &k_0 \frac{\partial T_0}{\partial z}\bigg|_{z=0} = k_1 \frac{\partial T_1}{\partial z}\bigg|_{z=0} \\ &T_1\big|_{z=L_1} = T_2\big|_{z=L_1} \\ &k_1 \frac{\partial T_1}{\partial z}\bigg|_{z=L_1} = k_2 \frac{\partial T_2}{\partial z}\bigg|_{z=L_1} \\ &T_2\big|_{z=L_1+L_2} = T_3\big|_{z=L_1+L_2} \\ &k_2 \frac{\partial T_2}{\partial z}\bigg|_{z=L_1+L_2} = k_3 \frac{\partial T_3}{\partial z}\bigg|_{z=L_1+L_2} \end{aligned} \quad (4)$$

By executing complex analysis and the Hankel transform for Eq. (2) using boundary conditions, the temperature distribution for the multi-layer model can be obtained.

$$T_0 = \int_0^\infty \beta d\beta J_0(\beta r) A e^{\delta_0 z} e^{i\omega t} \quad (5a)$$

$$T_1 = \int_0^\infty \beta d\beta J_0(\beta r) \times [B_1 e^{-\lambda_1 z} + B_2 \cosh(\delta_1 z) + B_3 \sinh(\delta_1 z)] e^{i\omega t} \quad (5b)$$

$$T_2 = \int_0^\infty \beta d\beta J_0(\beta r) \times [C_1 e^{-\lambda_2 (z-L_1)} + C_2 \cosh(\delta_1 (z-L_1)) + C_3 \sinh(\delta_1 (z-L_1))] e^{i\omega t} \quad (5c)$$

$$T_3 = \int_0^\infty \beta d\beta J_0(\beta r) D e^{-\delta_3 (z-L_1-L_2)} e^{i\omega t} \quad (5d)$$

where

$$A = B_1 + B_2$$

$$B_1 = -\frac{\lambda P_0 (1-R_1)}{8\pi k(\lambda_1^2 - \delta_1^2)} e^{-a^2\beta^2/4}$$

$$B_2 = \begin{bmatrix} \{(\chi_0 + k_1\lambda_1)\Gamma_1 - (\chi_2 + k_1\lambda_1)\chi_1 H_1 e^{-L_1\lambda_1}\} B_1 \\ +\{k_2\lambda_2 H_1 + \chi_1 H_2 \\ -(\chi_3 - k_2\lambda - 2)\chi_2 e^{-L_1\lambda_1}\} \times \chi_1 C_1 \end{bmatrix} /[-\chi_0\Gamma_1 + \chi_1\Gamma_2]$$

$$C_1 = -\frac{\lambda P_0 (1-R_1)(1-R_2)}{8\pi k(\lambda_2^2 - \delta_2^2)} e^{-\lambda_1 L_1} e^{-a^2\beta^2/4}$$

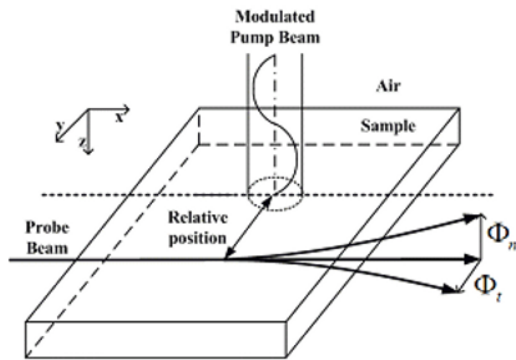

Fig. 2. Geometry of the transverse beam deflection (Φ_t) method.

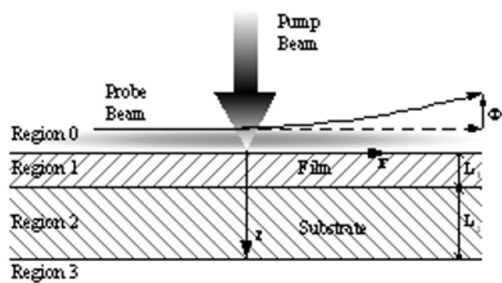

Fig. 3. Principle of measurement and theoretical models for the photothermal deflection method.

$$C_2 = -C_1 + B_1 e^{-\lambda_1 L_1} + B_2 \cosh(\delta_1 L_1) + B_3 \sinh(\delta_1 L_1)$$
$$C_3 = k_2\lambda_2 C_1 - B_1 k_1 \lambda_1 e^{-\lambda_1 L_1} + B_2 \chi_1 \sinh(\delta_1 L_1) + B_3 \chi_1 \cosh(\delta_1 L_1)$$
$$D = [-C_1 k_2 \lambda_2 e^{-\lambda_2 L_2} + B_2 \chi_2 \sinh(\delta_2 L_2) + B_3 \chi_1 \cosh(\delta_2 L_2)] / \chi_3 \tag{6a}$$

$$H_{1,2} = [e^{\delta_2 L_2}(\chi_2 + \chi_3) \pm e^{-\delta_2 L_2}(\chi_2 - \chi_3)]/2$$
$$\Gamma_{1,2} = [e^{\delta_1 L_1}(\chi_1 H_1 + \chi_2 H_2) \pm e^{-\delta_1 L_1}(\chi_1 H_1 - \chi_2 H_2)]/2$$
$$\delta_i^2 = \beta^2 + i\omega/\alpha_i$$
$$\chi_i = \delta_i k_i \qquad (i = 0,1,2,3) \tag{6b}$$

Eq. (1) can be modified to Eqs. (7) and (8) by using the result of the temperature analysis.

$$\Phi_t = -\frac{2}{n_0}\left[\frac{\partial n}{\partial t}\right]_{air} e^{i\omega t}\int_0^\infty \beta d\beta A e^{\delta_0 z}\sin(\beta y) \tag{7}$$

$$\Phi_n = \frac{2}{n_0}\left[\frac{\partial n}{\partial t}\right]_{air} e^{i\omega t}\int_0^\infty d\beta A g_0 e^{\delta_0 z}\cos(\beta y) \tag{8}$$

3. Experimental apparatus

Fig. 4 shows the schematic diagram of the experimental apparatus. The pump beam, as a heating source, is a continuous Ar-ion laser with a wavelength of 488nm and a diameter of 1.4mm with Gaussian distribution. The pump beam is modulated as a sine wave through the acoustic-optic (A-O) modulator, which is controlled by a lock-in amplifier. This modulated beam is focused on the surface of the sample with a diameter of 110-120 μm. After passing through the A/O modulator, mirrors, the expander, the convex lens (FL500), and the iris pin-hole, the beam reaches the surface of the sample with 35% of its power. It is critically important for the pump beam to be perpendicular to the surface of the sample. The probe beam is generated by a He-Ne laser with a wavelength of 633nm and 5mW power. The line of the probe beam is kept parallel to the surface of the sample. The distance between the center line of the probe beam and the surface of the sample is set to 100 μm. Through the convex lens (FL200), the probe beam is focused to be about 70 μm in diameter near the surface of the sample. The probe beam is filtered by an optical band-pass filter before it enters the two-dimensional position sensor. The signal from the position sensor is coupled with the amplifier and measured by the lock-in amplifier. The alignment of the laser and the dial gauge are used to record the position and tilting angle of the sample. When a sample is replaced, the replacement sample can be set to the same position and tilting angle as the original sample.

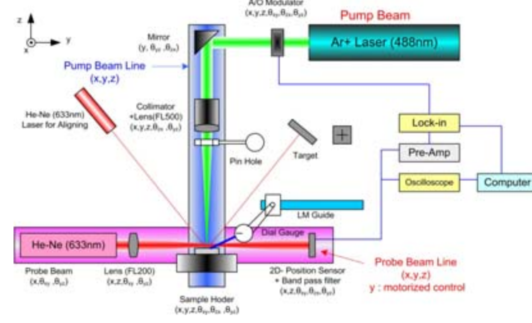

Fig. 4. Schematic diagram of the experimental setup for the photothermal deflection method.

For more accurate measurement, the probe-beam laser and the two-dimensional position sensor are installed on the same rail fixed on the linear motor-driven vertical stage. The motor-driven stage is connected to the computer and controlled with a resolution of 0.1 μm. Since the sample is not moved during measurement, the relative position [15], that is, the distance between the center of the spot of the pump beam and the center line of the probe beam, is controlled by the motion of the probe-beam line rail.

Prior to the main experiment, the measurement for pure metals was performed to verify the reliability of the experimental setup. Cu with 0.4mm thickness and Zn with 1mm thickness were selected as the reference materials.

For the samples used in the main experiment, Al film, Si_3N_4 film, and TiO_2 film deposited on Corning 7740 glass substrates with a thickness of 5mm were used. Al film and Si_3N_4 film were deposited with thicknesses of 0.2 μm, 0.4 μm, 0.6 μm, 0.8 μm, and 1 μm. TiO_2 film was deposited with thicknesses of 0.48 μm, 0.6 μm, and 1 μm. In the case of Al film samples, the purity of the deposited Al film was 80.53%, as a result of the reduction in purity that occurred during the process of deposition. The thermal conductivities of bulk Si_3N_4 film and TiO_2 were 35.0 and 11.9 W/mK, respectively [19]. For each sample, the transverse phase difference of the probe beam was measured by changing the relative position of the pump beam and the probe beam. The thermal conductivities were

determined by comparing the measured results with theoretical values.

4. Results and discussion

4.1 The effect of modulation frequency

This study investigated the optimal condition of the modulation frequency of the pump beam laser to yield more accurate measures. Modulation frequency is related to the thermal diffusion length ($L_{th} = \sqrt{\alpha / \pi f}$) of the sample. In general, a more accurate measurement is conducted under 'thermally thick' conditions, that is, when the thermal diffusion length is thinner than the sample. The lock-in amplifier used in this measurement removed the noise from the source of electric power at 50Hz, 60Hz, and multiples of these two frequencies.. To search for the optimal frequency and obtain a signal with high S/N ratio, the signal magnitude was measured for frequencies ranging from 5Hz to 3000Hz; the range of 200–400Hz was identified as the optimal condition. In the measurement for Al and TiO_2 film samples, 220Hz was used as the modulation frequency. Because Si_3N_4 has a very low optical absorption coefficient, the measurement for Si_3N_4 films was conducted at 20Hz so that the samples could absorb more light energy. However, the thermal diffusion length of Si_3N_4 film was not larger than the thickness of the sample because the thermal conductivity of Si_3N_4 was relatively low.

4.2 Measurement for pure metal

Prior to the measurement for film samples, the verification of the measurement technique was carried out through the measurement for the bulk materials, Cu and Zn, with 0.4mm and 1mm thickness, respectively. Table 1 shows the experimental results of the measurement of conductivities and the corresponding figures from the literature. The measured conductivity for Cu was 401.2W/mK, compared with the value of 398W/mK that is reported in previous research. The conductivity of Zn was measured as 113.6W/mK, compared with the value of 113W/mK reported in previous research.. The relative errors for the Cu and Zn measurements were 0.8% and 0.5% , respectively. A relative error of less than 1% confirmed that the experimental setup was highly reliable for the measurement of thermal conductivity.

Table 1. Measures of thermal conductivity for pure metal. (M: Measured value, L: Literature value)

	M (W/mK)	L (W/mK)	R.E. (%)
Cu	401.2	398	0.8
Zn	113.6	113	0.5

Table 2. Measures of thermal conductivity for thin film.

Thickness(㎛)	80.53% Al film		Si_3N_4 film	
	k(W/mK)	Values normalized by data for 1 ㎛ (%)	k(W/mK)	Values normalized by data for 1 ㎛ (%)
1	142	100	32.4	100
0.8	141.5	99.6	31.6	97.5
0.6	137.6	96.9	30.9	95.4
0.4	133.6	94.1	30.2	93.2
0.2	130.6	92	27.5	84.9

Thickness(㎛)	TiO_2 film	
	k(W/mK)	Values normalized by data for 1 ㎛ (%)
1	11.1	100
0.6	9.6	86.5
0.48	9.2	82.9

4.3 Measurement for thin film

The measurement of thermal conductivity for thin film was conducted to investigate the variations in thermal conductivities with thickness. Conductivities were measured for Al and Si_3N_4 films with 0.2 ㎛, 0.4 ㎛, 0.6 ㎛, 0.8 ㎛, and 1 ㎛ thickness and for TiO_2 films with 0.48 ㎛, 0.6 ㎛, and 1 ㎛ thickness. (see Table 2 for the results of the measurement. Conductivities for all kinds of sample decreased with decreasing thickness. This means that in thin samples, the boundary surface interferes with the motion of phonons or electrons for heat transfer. To further investigate the effect of thickness further, each measurement was normalized by the corresponding value for the sample with 1 ㎛ thickness (see Fig. 5 for the normalized conductivities). Based oh the figure, the thermal conductivities of Al film are affected when the thickness is below 0.6 ㎛. It must be noted as well that the phonons in Si_3N_4 films appear to be strongly restricted at thicknesses below 0.2 ㎛, resulting in the steep slope. For TiO_2 films, the thermal conductivity decreases at a relatively constant rate with decreasing thickness.

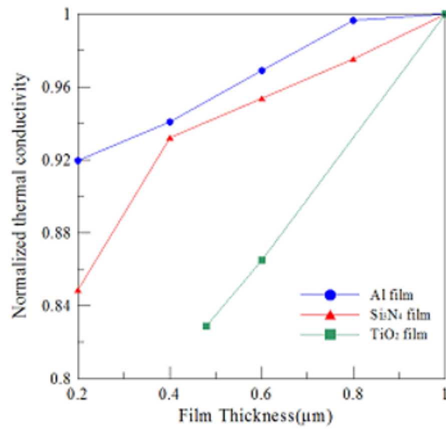

Fig. 5. The variation of the normalized thermal conductivity with thickness.

5. Conclusion

In this study, the thermal conductivities of thin films with submicroscale thickness were measured using the photothermal deflection method. Accurate equipment, optical units, and stages resulted in a high reliability of measurement. The measurement for pure metals, namely, Cu and Zn, was conducted to verify the experimental setup (the relative errors were less than 1%). After the verification, the thermal conductivities were measured for Al, Si_3N_4, and TiO_2 thin films with varying levels of submicroscale thickness from 1 μm down to 0.2 μm. The variation of thermal conductivity with thickness was observed. Furthermore, the optimal condition of the modulation frequency, in relation to the thermal diffusion length of the sample, was identified to optimize the measurements. The results showed that for submicroscale films, the thermal conductivities decreased as the film thickness decreased, thereby revealing a phenomenon about heat transfer at the microscale.

Acknowledgments

This research was financially supported by the Ministry of Knowledge Economy (MKE) and the Korea Industrial Technology Foundation (KOTEF) through the Human Resource Training Project for Strategic Technology and by the Ajou Universtiy Research Fellowship 2007 (Grant No. 20072650)..

Nomenclature

a : Radius of the pump beam [m]
f : Modulation frequency [Hz]
J_0 : Zero-order Bessel function
k : Thermal conductivity [W/mK]
L : Sample thickness [m]
L_{th} : Thermal diffusion length [m]
n : Refractive index
P : Power of the pump beam [W]
Q : Intensity of the heat source [W/m^3]
R : Reflectivity
T : Fluctuating temperature [K]
t : Time [sec]

Symbols

Φ : Deflection angle [deg]
α : Thermal diffusivity [m^2/s]
β : Integration Variable
λ : Optical absorption coefficient [1/m]
ω : Angular frequency [1/s]

Subscript indices

n : Direction of the normal
t : Direction of the tangent
0 : Front-gas region
1 : Thin-film region
2 : Substrate region
3 : Rear-gas region

References

[1] R. W. Powell and R. E. Taylor, Multi-property apparatus and procedure for high temperature determinations, *Rev. Int. Hautes Temp. et Refract.*, 7 (1970) 298-304.
[2] R. E. Taylor, W. D. Kimbrough and R. W. Powell, Thermophysical properties of Tantalum, Tungsten and Tantalum-10wt. percent Tungsten at high temperatures, *J. Less-common Metals*, 24 (1971) 369-382.
[3] R. E. Taylor, *Determination of thermophysical properties by direct electric heating*, *High Temp.-High Press.*, London, UK, (1981).
[4] A. Cezairliyan, M. S. Morse and C. W. Beckett, Measurement of melting point and electrical resistivity of molybdenum by a pulse heating method, *Rev. Int. Hautes Temp. et Refract*, 7 (1970) 382-388.
[5] A. Cezairliyan, Design and operational characteristics of a high speed system for the measurement of thermophysical properties at high temperatures, *J.*

es. NBS, 75C (1) (1971) 7-18.

[6] A. Cezairliyan and A. P. Miller, Specific heat capacity and electrical resistivity of a Carbon-Carbon composite in the range 1500-3000K by a pulse heating method, *Int. J. Thermophys*.1 (3) (1980) 317-330.

[7] J. A. Sell, *Photothermal investigations of solids and fluids, Academic Press*, Boston, USA, (1989).

[8] D. G.Cahill, M. Katiyar and J. R. Abelson, Thermal conductivity of a- Si:H thin films, *Phys Rev. B.* 50 (9) (1994) 6077-6081.

[9] J. P. Hiernaut, F. Sakuma and C. Ronch, *Determination of the melting point and of the emissivity of refractory metals with a six-wavelength pyrometer*, *High Temp.-High Press*., London, UK, (1989) 11-16.

[10] T. Baba, T. Arai and A. Ono, Uniformalization of laser beam profiles using an optical fiber, *Proc. 7t]h Japan Symposium on Thermophysical properties*, Tsukuba, Japan (1986) 235-238.

[11] T. Arai, T. Baba and A. Ono, *Thermographic investigation of laser flash diffusivity measurement, High Temp.-High Press.,* London, UK, (1987).

[12] A. Salazar, A. Sanchez-Lavega and J. Fernandez, Theory of thermal diffusivity determination by the “mirage” technique in solids, *J. Appl. Phys*., 65 (11) (1989) 4150-4156.

[13] A. Salazar, A. Sanchez-Lavega and J. Fernandez, Thermal diffusivity measurements in solids by the mirage technique: experimental result, *J. Appl. Phys*., 69 (3) (1991) 1216-1223.

[14] P. Jeon, E. Lee, K. Lee and J. Yoo, A theoretical study for the thermal diffusivity measurement using photothermal deflection scheme, *Energy Engg. J.* 10 (1) (2001) 63-70.

[15] K. J. Lee, *The measurement of thermal conductivity for thin film and temperature effects on thermal diffusivity for metals, Ph. D. thesis*, Ajou University, (2005).

[16] X. Chen, Thermal diffusivity of surface-microstructured silicon measured by photothermal deflection technique, *Mater. Lett.* 60 (2006) 63-66.

[17] Celeste B. Reyes, *Thermal wave measurement of thermal diffusivity of solids, Ph. D. thesis*, Wayne State University, (1988).

[18] M. N. Ozisik, *Heat Conduction, Wiley Interscience*, New York, USA, (1993).

[19] J. F. Shackelford, *CRC materials science and engineering handbook, CRC Press*., New York, USA, (1994).

Jaisuk Yoo received his B.S. and M.S. degree in Mechanical Engineering in 1980 from Seoul National University. He received his Ph.D. in Mechanical Engineering in 1984 from University of California, Berkeley. He currently works in Division of Mechanical Engineering, Ajou University as a professor since 1985. His research interests are nano fluidics, micro scale heat transfer and optical property measurement.

Hyun Jung Kim received his B.S. and M.S. degree in Mechanical Engineering in 1996 from Hanyang University. He received his Ph.D. in Mechanical Engineering in 2001 from Texas A&M University. He currently works in Division of Mechanical Engineering, Ajou University as an associate professor since 2003. His research interests are nano fluidics, optical property measurement, micro scale heat and mass transfer and measurement with Micro PIV, LIF.